ELSEVIER

Thin Solid Films 265 (1995) 74–83

thin solid films

X-ray diffraction structural analysis of Langmuir–Blodgett films using a pattern recognition approach

Elisabetta Maccioni [a], Paolo Mariani [a,*], Franco Rustichelli [a], Hervé Delacroix [b], Vladimir Troitsky [c], Antonio Riccio [c], Agata Gambacorta [d,e], Mario De Rosa [d,e]

[a] *Istituto di Scienze Fisiche, Facoltà di Medicina, Università di Ancona, via Ranieri 65, 60131 Ancona, Italy*

[b] *Centre de Génétique Moléculaire, Laboratoire Propre du CNRS, Associé à l'Université P. et M. Curie, 91191 Gif-sur-Yvette, France*

[c] *Consorzio Technobiochip, via Roma 28, 57030 Marciana (Livorno), Italy*

[d] *ICMIB, via Toiano 2, Arco Felice, Napoli, Italy*

[e] *Istituto di Biochimica delle Macromolecole, Facoltà di Medicina, II Università di Napoli, via Costantinopoli 16, 80136 Napoli, Italy*

Received 15 November 1994; accepted 28 March 1995

Abstract

A new approach for the analysis of X-ray diffraction patterns to obtain the structure of Langmuir–Blodgett (LB) films is reported. In particular, to solve the ''phase problem'' we apply a direct method, essentially a pattern recognition approach, which was recently proposed to determine without assumptions the structure of liquid-crystalline phases. This approach is used to analyse two different types of samples, namely LB films of fatty acid salts and of bipolar lipids extracted from thermoacidophilic archaeon *Sulfolobus solfataricus*. As a result, the electron density profiles allow us to fully characterize the molecular arrangement in both the investigated films.

Keywords: Biomaterials; Langmuir–Blodgett films; Structural properties; X-ray diffraction

1. Introduction

The Langmuir–Blodgett (LB) method of successively transferring monomolecular layers from the air–water interface onto a solid substrate is a useful technique for the preparation of films of amphiphilic molecules [1]. The peculiar structures which can be obtained have great technological and theoretical interests. They are considered as simple models to investigate the properties of two-dimensional biological [2,3] and artificial [4] systems. Moreover, the electrical, optical and chemical properties that such molecular assemblies show (see for example Refs. [5–7]) as well as the complex structures which could be created (the so-called 'superlattices') make them suitable for developing devices which cannot be made by traditional techniques [8–10].

A growing technological interest has been very recently devoted to the production of LB films of bipolar isoprenoid ether lipids [11]. These molecules are the structural components of the cellular membrane of Archaea, a phylogenetically coherent separate group of micro-organisms, that differ from Eubacteria and Eukarya. Archaea comprises a variety of extremophilic bacteria that live segregated into a few peculiar ecological niches characterized by extreme environmental parameters, such as saturated brine for halophiles, strictly anaerobic environments for methanogens, and thermal habitats for extreme thermophiles [12,13]. The archaeal membrane lipids are mainly composed of saturated isoprenic chains of different lengths, in ether linkages to glycerol carbons with the sn-2,3 configuration, instead of fatty acyl chains which are often unsaturated and are esterified to glycerol at carbons sn-1,2 [14–16]. These compounds have an unprecedented molecular architecture; in fact, while classic lipids are monopolar amphipatic molecules, archaeal lipids are bipolar amphipatic molecules characterised by the presence of two polar heads and of an hydrophobic moiety that is practically twice the average length of the aliphatic components of classic ester lipids [17,18]. Considering their unique molecular structure, lipids from Archaea are promising for the creation of an artificial media stable at extreme conditions just destined by nature for the incorporation of some functional molecules such as proteins.

In this paper, we focus on the determination of the profile of the electron density distribution across LB films, as obtained by the analysis of X-ray diffracted intensities. In particular, it has been recently reported that in the case of liquid crystalline lyotropic structures, the electron density

* Corresponding author. Tel. +39.71.220.4608, Fax +39.71.2204.605.

SSDI 0040-6090(95)06620-9

distributions could be calculated ab initio by using a pattern recognition approach which gives a direct solution to the crystallographic phase problem [19]. We show here that the same approach could be extended from lyotropic systems, which are characterised by an intrinsically low resolution (typically about 1.0–1.5 nm), to LB films, which on the contrary could be very ordered [20]. Two kinds of systems will be considered: the first consists of a series of well known LB films made of fatty acid salts (experimental resolution from 0.4 to 0.2 nm), while the second is a series of LB film made of bipolar lipids. In this case, the experimental resolution is low, as it appears very difficult to produce ordered films [11].

2. Experimental details

2.1. Purification of archaeal lipids

We prepared LB films of a mixture of two complex membrane lipids (Fig. 1), synthetically named Phospho 2, extracted from the thermoacidophilic archeon *Sulfolobus solfataricus*, a micro-organism that grows optimally at 87 °C and pH 3. These membrane lipids are based on two series of tetraether core lipids, named caldarchaeol (Figs. 1(a)–1(c)) and nonitolcaldarchaeol (Figs. 1(a′)–1(c′)). The investigated mixture contains 90% of the phospho-*myo*-inositol-β-D-glucopyranosyl derivative of nonitolcaldarchaeol and 10% of the phospho-*myo*-inositol-β-D-galactopyranosyl-β-D-gluco-pyranosyl derivative of caldarchaeol.

S. solfataricus (DSM 1617) was obtained from the Deutsche Sammlung von Mikroorganismen und Zellkulturen GmbH (Braunschweig). The microorganism was grown at 87 °C in a 100 l fermenter containing 90 l of medium as described by De Rosa et al. [21]. Cells were harvested in the late stationary growth phase of incubation (48 h) by centrifugation. The dried cells were extracted continuously with a Soxhlet apparatus for 12 h with chloroform/methanol (1:1 v/v) and then with methanol/water (1:1 v/v). The total lipid extract was purified on silica gel (Merck Kieselgel 230–400 mesh) column, eluted under pressure using eluents of increased polarities: chloroform, chloroform/methanol (85:15 v/v), chloroform/methanol (65:25 v/v), chloroform/methanol/water (65:25:4 by vol). Phospho 2 was recovered in the chloroform/methanol/water fraction. The relative amount of the two lipids is based on the caldarchaeol/nonitolcaldarchaeol ratio obtained by acid hydrolysis of Phospho 2 (6 N HCl at 100 °C for 72 h) [22].

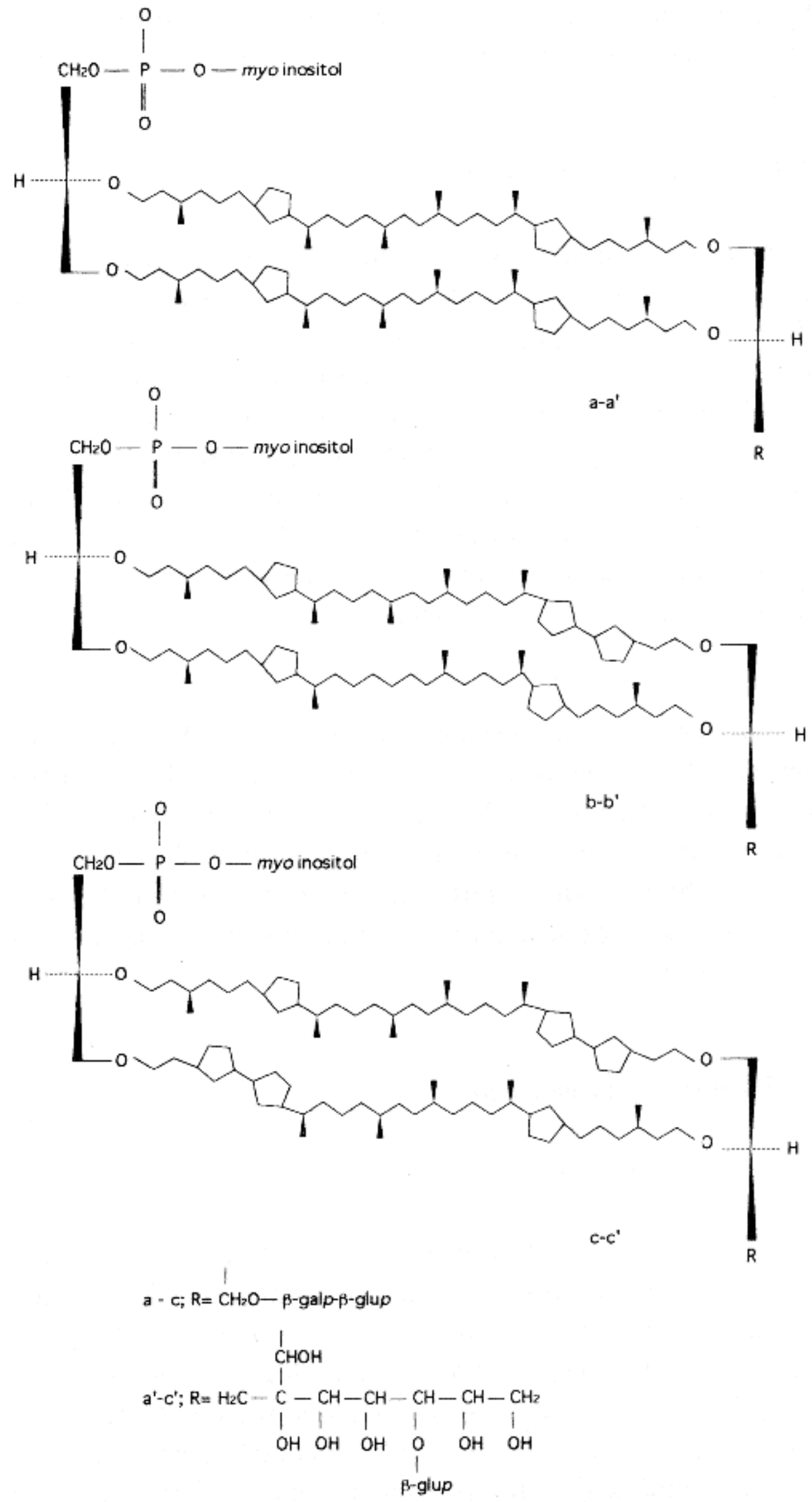

Fig. 1. Structures of the phospho-*myo*-inositol-β-D-galactopyranosyl-β-D-glucopyranosyl derivative of caldarchaeol ((a)–(c)) and of the phospho-*myo*-inositol-β-D-glucopyranosyl derivative of nonitolcaldarchaeol ((a′)–(c′)). Caldarchaeols and nonitolcaldarchaeols are the basic components of the complex membrane lipids of the iperthermophilic archeon *Sulfolobus solfataricus*. The lipid fraction Phospho 2 has the following tetraether composition: a–a′, 60%; b–b′, 30%; and c–c′, 10%.

2.2. Deposition of the films

Fatty acid salt monolayers were formed with a LB-MDT-4000 Langmuir trough. Thrice-distilled water (metal distiller and quartz bi-distiller) was used for subphase preparation. Solutions of fatty acids in benzene (0.5 mg ml^{-1}) were spread over aqueous subphases 5×10^{-5} M $Pb(NO_3)_2$ at pH 6.0, 10^{-3} M $TlNO_3$ at pH 9.8 and 10^{-4} M $CdCl_2$ at pH 7.2 for depositing lead, thallium and cadmium fatty acid salts, respectively. For low-angle X-ray scattering experiments, multilayers were deposited on hydrophobic silicon substrates treated by dimethyldichlorosilane. Deposition was carried out with a rate of 2 mm min^{-1} at surface pressure of 27 mN m^{-1} by the vertical lift technique.

Phospho 2 lipid was dissolved in a $CHCl_3$/MeOH/water (65/25/4 by vol.) mixture at concentration of 0.33 mg ml^{-1}. An aqueous subphase of pH 6.9 was used. For low-angle X-ray scattering experiments, 50 monolayers were deposited on

hydrophobic silicon substrates by the horizontal lift technique at a surface pressure of 27 mN m^{-1}. Water drops were removed by argon streaming.

2.3. X-ray diffraction experiments

X-ray experiments were performed on a Rigaku Denki RV300 rotating anode generator equipped with a powder diffractometer: the goniometer radius was 185 mm and divergence and receiving slits of 0.05 mm (ca. 0.03°) were used. Ni-filtered Cu Kα radiation ($\lambda = 0.154$ nm) was produced with accelerating voltages of 40 kV at 200 mA. Data were collected with a proportional counter by the θ–2θ method and corrected for Lorentz and polarization effects after the method of Blaurock and Worthington [23] in a way appropriate for planar multilayered structures [20]:

$$I(h) = hI_m[1 + (\cos 2\theta)^2]/2 \quad (1)$$

where $I(h)$ are the corrected intensities, I_m the intensities measured from the peak integral areas, h the order of reflection and θ the Bragg angle. The scattering of the hydrophobic silicon substrate was measured separately and subtracted. The error in the intensity determination did not exceed 5%. The methods used for structure determination are discussed in a next section.

3. Results and discussion

3.1. Surface pressure isotherms

As an example of results obtained in the case of fatty acid salts, the surface pressure isotherm relative to a Pb stearate monolayer at 22 °C on the water surface is presented in Fig. 2. As expected [24], changes in the slope of the isotherm revealed the existence of three different regions corresponding to the gas/LC coexistence plateau and to the two-dimensional liquid and solid phases. By extrapolating to zero surface pressure the compressed state isotherm portion, the area available for one molecule at the air–water interface has been determined: the areas per molecule relative to the different fatty acids are presented in Table 1.

The surface pressure isotherm obtained at the same temperature for the Phospho 2 is presented in the lower part of Fig. 2: the area occupied by one molecule in the compressed state at zero surface pressure is about 0.98 ± 0.02 nm^2. Considering [11] that the minimum cross-section of one isoprenoid chain is about 0.25 nm^2, the U-shaped conformation of the bipolar molecules at the air–water interface with approximately vertical arrangement of the tails (see Fig. 3(a)) appears very probable. In this condition, the bend of the isopranyl chains somewhere in the middle position happens in such a manner that the chains result closely packed in the monolayer and that both headgroups (which are characterized by a strong and approximately similar hydrophilicity) could interact with water. It is obvious that such situation

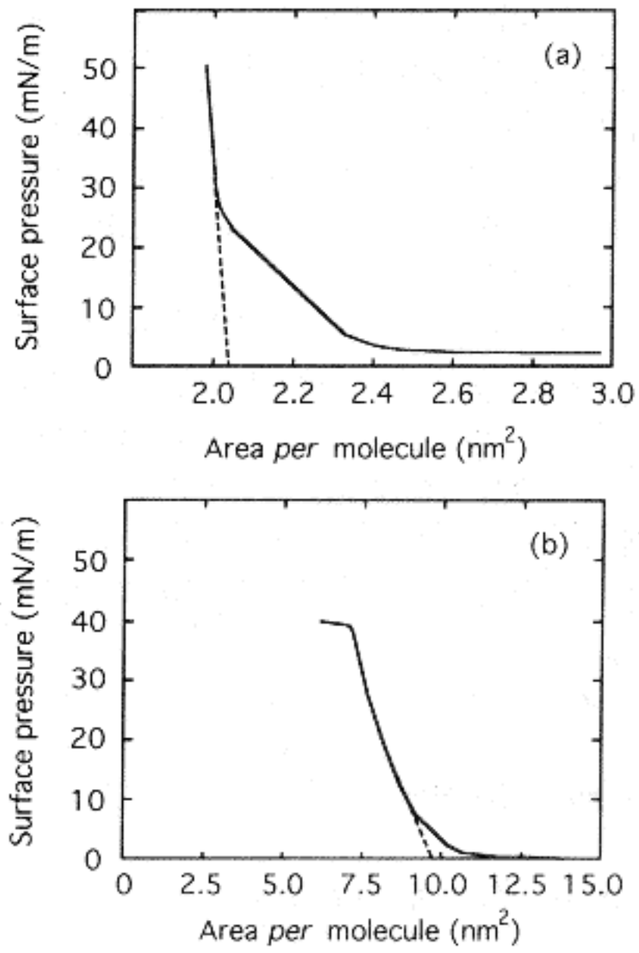

Fig. 2. Surface pressure isotherms at 22 °C of a Pb-stearate monolayer on water (a, upper part) and of a Phospho 2 monolayer on water (b, lower part). The dashed lines indicate the areas per molecule which have been determined.

cannot be distinguished from that corresponding to strongly tilted molecules in the fully extended conformation (see Figs. 3(b) and 3(c)). However, very recently X-ray reflectivity measurements on the same system at the air–water interface strongly suggest the U-shaped conformation [25].

3.2. X-ray diffraction data

3.2.1. Fatty acid salt LB films

The measured X-ray diffraction patterns of fatty acid salt LB films contain typically from 12 to 25 Bragg reflections, whose spacing ratios in the order 1:2:3:4... clearly indicate the one-dimensional lamellar symmetry[1] in correspondence to the packing of molecular layers in ''stacks'' [26]. The X-ray diffraction profile observed in the case of Pb stearate is reported as an example in Fig. 4.

From the peak positions and by using the classical Bragg equation, the dimension of the unit cell has been determined: for the different investigated films they are reported in Table 1. It can be easily observed that the difference in bilayer thicknesses is of about 0.5 nm for the salts of neighbouring fatty acids: this value rightly corresponds to the twice of the projection of two C–C bonds on the molecular axis direction (one link of the hydrocarbon chain on the molecular axis being in fact about 0.127 nm). In particular, as the preparation method ensures that the layers are centrosymmetric with two

[1] In this symmetry system in fact the equation that defines the spacings of reflections is [26]:

$$s(h) = h/D$$

where $s(h)$ is the reciprocal peak position (nm^{-1}), h is the Miller index of the reflection and D the unit cell dimension (nm).

Table 1
Structural parameters relative to the investigated LB films

	D (nm)	α (°)	A (nm^2)
Myristic	3.80	13.0	0.192
Palmitic	4.41	11.5	0.205
Stearic	4.90	16.0	0.203
Arachidic	5.39	15.7	0.205
Behenic	5.90	14.7	0.205
Lignoceric	6.40	14.1	0.190
Phospho 2	5.01	–	0.980

Reported data are for Pb salts. D is the unit cell dimension and α is the angle of tilt of the chains with respect to the normal to the bilayer surface. A refers to the areas per molecule determined from surface pressure isotherms. For the other investigated ions, the spacings for the same acid may differ by about 0.01–0.03 nm, while the differences in the tilt angles and in the areas per molecule are inside the experimental error.

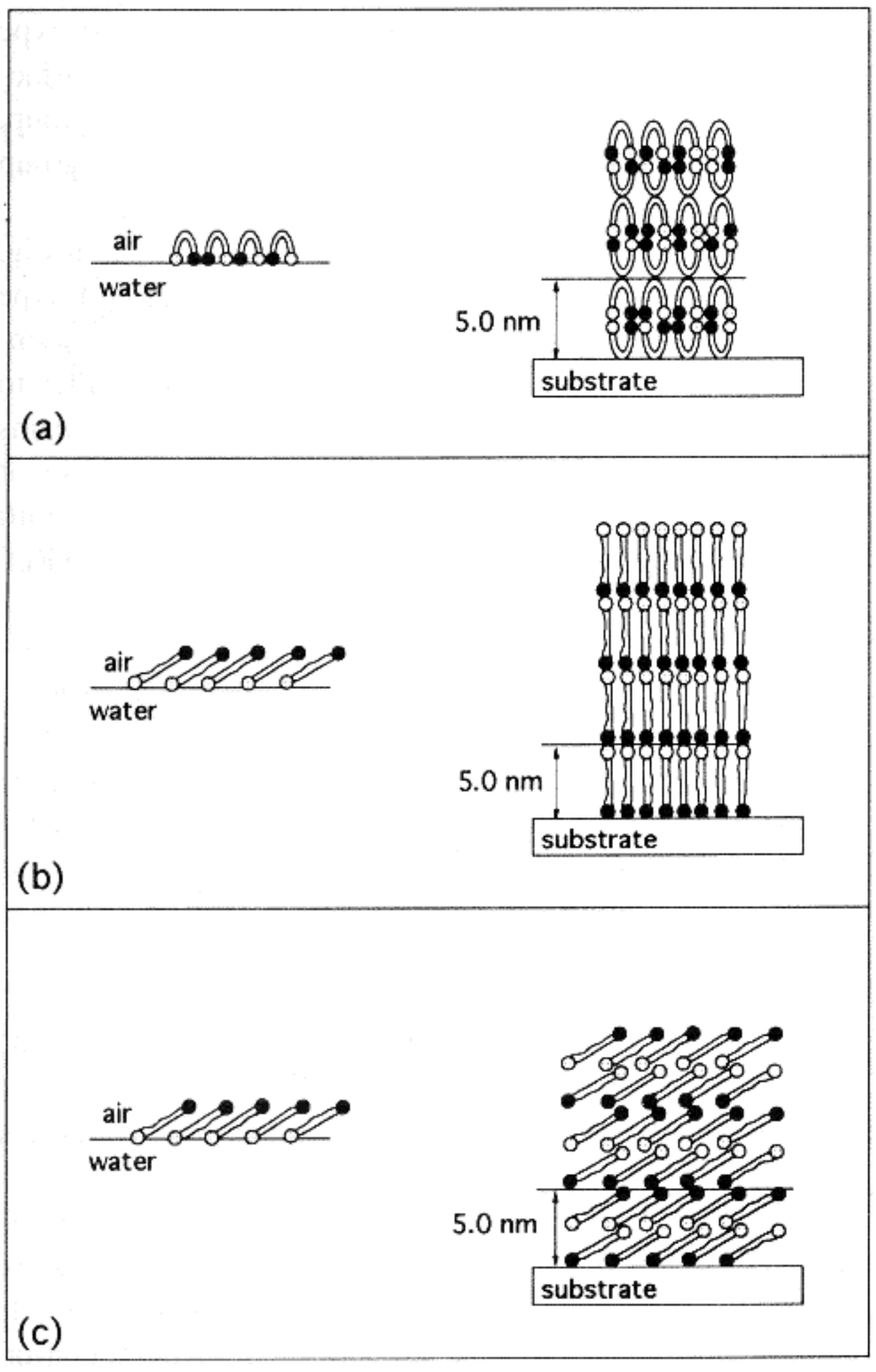

Fig. 3. Schematic structural models for the conformations eventually assumed by the Phospho 2 bipolar lipid molecules at the air–water interface (left side) and on the LB films (right side). The gray and black circles represent the two different polar headgroups; the wriggles represent the hydrocarbon chains. The U-shaped conformation is represented in the frame (a), while in the lower frames are depicted two possible fully extended polar (b) and tilted (c) conformations.

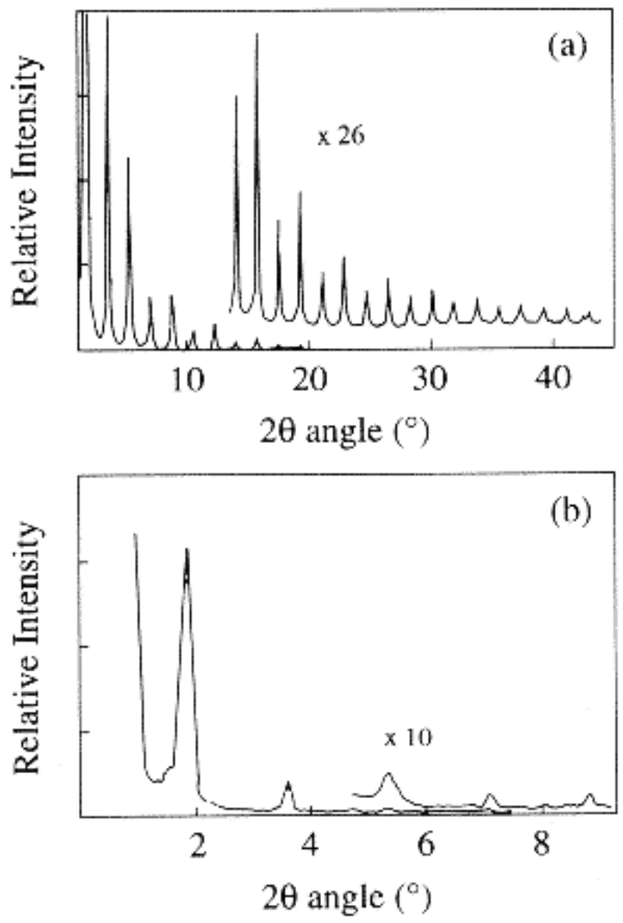

Fig. 4. X-ray diffraction patterns of 40 monolayers of Pb stearate (a, upper part) and of 50 monolayers of Phospho 2 (b, lower part). Note that in the two profiles the 2θ angle axes have different ranges.

molecules in the unit cell projection to the z axis (i.e. the axis normal to the LB film planes), the comparison between the length of the molecules with the dimensions of the cell clearly indicates that the hydrophobic chains deviate slightly from the z direction. The angle of tilt of the chains with respect to the normal to the bilayer surface can be calculated by using the following equation:

$$\cos \alpha = D/2L \quad (2)$$

where D is the unit cell dimension and L is the length of the molecule with fully extended chain. As already reported (see for example Ref. [24]), for all samples investigated we found a tilt angle of about 15°.

Finally, the moduli of the structure factors relative to the Bragg peaks observed in the X-ray diffraction profiles for three different fatty acid Pb salts are reported in Table 2.

3.2.2. Bipolar lipid LB films

The measured X-ray diffraction patterns relative to Phospho 2 LB films (see for example the one reported in Fig. 4) show, in the better cases, from 4 to 5 Bragg reflections [11] which corresponds to an experimental resolution of about 1 nm. This is not surprising, as an intrinsically low resolution is expected considering that the production of ordered bipolar lipid films is not easy, both using a vertical or horizontal lift technique and even if, during the production, the system is controlled as much as possible. This fact has been explained considering that monolayers of this compound interact with water more strongly than with each other [11]. However, the spacing ratios in the order 1:2:3:4... confirmed the one-dimensional lamellar symmetry. The moduli of the structure factors relative to the measured X-ray diffracted intensities are reported in Table 2.

Table 2
Moduli of the structure factors relative to the measured X-ray diffracted intensities for some investigated LB films

	Pb stearate	Pb arachidate	Pb behenate	Phospho 2
D (nm)	4.90	5.39	5.90	5.01
$c_{v,pol}$	0.064	0.058	0.054	0.276
$\langle(\Delta\rho)^4\rangle^*$	13.69	15.30	16.58	2.00
$F(1)$	0.468	0.428	0.339	0.622
$F(2)$	0.268	0.222	0.242	0.288
$F(3)$	0.251	0.245	0.275	0.129
$F(4)$	0.153	0.145	0.189	0.081
$F(5)$	0.175	0.211	0.211	0.084
$F(6)$	0.113	0.154	0.158	0.0
$F(7)$	0.143	0.183	0.187	–
$F(8)$	0.102	0.131	0.132	–
$F(9)$	0.105	0.132	0.175	–
$F(10)$	0.066	0.114	0.108	–
$F(11)$	0.079	0.134	0.123	–
$F(12)$	0.052	0.070	0.123	–
$F(13)$	0.062	0.045	0.106	–
$F(14)$	0.045	0.057	0.099	–
$F(15)$	0.055	0.064	0.0	–
$F(16)$	0.046	0.045	–	–
$F(17)$	0.050	0.040	–	–
$F(18)$	0.033	0.040	–	–
$F(19)$	0.047	0.0	–	–
$F(20)$	0.041	–	–	–
$F(21)$	0.042	–	–	–
$F(22)$	0.039	–	–	–
$F(23)$	0.038	–	–	–
$F(24)$	0.034	–	–	–
$F(25)$	0.0	–	–	–

The $c_{v,pol}$ refers to the volume concentration of the lipid polar headgroups in the case of Phospho 2 and of the Pb ion in the case of fatty acid salts (see text). The partial CH_3 and CH_2 volumes have been derived from Ref. [33] and the ion volumes from Ref. [24]. For bipolar lipids, the polar and paraffinic volumes have been derived from Ref. [34]. The intensities of each experiment have been normalised such that $\Sigma I(h) = 1.0$. Other symbols and notations as in Table 1 and in the text.

The dimension of the unit cell, as determined from the peak positions, is reported in Table 1. It is interesting to observe that 5 nm corresponds to the length of a fully extended Phospho 2 molecule [11,17,18]. Therefore, a first structural model for the film corresponds to the stacking of monolayers made of fully extended lipid molecules, strictly perpendicular to the layer surface. As it can be seen in Fig. 3(b), this model assumes strong changes of the structure during the process of deposition. Indeed, comparing the chain cross-section and area per molecule presented above, it is evident that the chains of extended molecules in the monolayer must be tilted by 50–60°. Therefore, the area per molecule in the deposited film must decreases practically twice with respect to that in the monolayer at the air–water interface (Fig. 3(b)). During deposition, such change of area per molecule cannot occur, so this model appears hardly probable. However, such recrystallization has been discovered in some LB films to coincide with an ''interdigitation'' process [27]: during the deposition of every even monolayer, chains of molecules penetrate between the chains of the molecules of a previously deposited odd monolayer.

Considering the simple model depicted in Fig. 3(b), it could be observed that two extreme situations could arise: in the first case the molecular packing is polar, in the sense that the two different lipid headgroups are preferentially located in alternate sublayers. As a consequence, the projection of the structure on the z direction is not-centrosymmetric. By contrast, if at the air–water interface there is not a preferential orientation of the extended molecules, the resulting molecular packing in the deposited layer will be non-polar, and consequently the projection of the structure on the z direction will be centrosymmetric.

The observed unit cell dimension is also compatible with a bilayer centrosymmetric structure, each monolayer being made of molecules showing the U-shaped conformation, as reported in Fig. 3(a). It has in fact been observed [11] that the thickness of such monolayers is indeed 2.5 nm. As was mentioned previously, this conformation is the more probable at the air–water interface and then in this case usual Y-type deposition takes place: Phospho 2 behaves as a usual surfactant compound, which consists of one hydrophobic group, located at one side, and one, even complex, hydrophilic group located at the opposite side of the molecule.

A third possibility for the film structure is shown in Fig. 3(c). As in the case presented in Fig. 3(a), a film of Y-type is supposed to be deposited so that the structure is centrosymmetric. Molecules in the extended form are strongly tilted to the substrate plane, so that the area per molecule remains approximately equal to 0.98 nm^2. Note that the possibility of Y-type film formation under deposition by the horizontal lift technique can be understood from the model proposed in Ref. [28].

3.3. Structure analysis by pattern recognition approach

In order to characterise the arrangement of molecules within the layer, the electron density profiles across the LB films (z direction) have been determined. The electron density distribution along the z direction, $\rho(z)$, can be written as [26]:

$$\rho(z) = \sum_{h=-\infty}^{\infty} F(h) \exp\left(-2\pi i h \frac{z}{D}\right) \qquad (3)$$

were $F(h)$ is the structure factor of the reflection with order h.

However, in both the investigated systems the 1-D unit cell can be considered to be centrosymmetric. For fatty acid salts, this fact is a direct consequence of the deposition process. In the case of bipolar lipids, for which three molecular conformations at the air–water interface have been considered, this fact depends on the deposition process (see the structural models shown in the Figs. 3(a) and 3(c)), or it depends on the low experimental resolution and on the rather similar electron densities of the two polar groups (see the model reported in Fig. 3(b)). Therefore, the phase problem is

reduced to a sign problem, i.e. to the determination of the correct signs of all the observed structure factors (we will refer to the sign combinations as φ-sets).

For searching the correct combination of signs, we resort to a pattern recognition approach recently proposed to solve the structure of lyotropic liquid crystalline phases [19,29–31]. This approach is based upon the axiom that the histogram of the electron density map [2] $H(\Delta\rho)$ is an extensive property of the system, being strongly dependent upon chemical composition rather than on physical structure [19]. In order to select the best φ-set, all the sign combinations compatible with the experimental data are generated (the φ-set list) and the histograms relative to the corresponding electron density maps are calculated. Among these histograms, the best one must be then selected. From a practical viewpoint, only one single parameter is found to provide the basis for the screening: the $\langle(\Delta\rho)^4\rangle$, i.e. the fourth moment of the histogram of the normalised electron density distribution[2]. Two strategies have been adopted for the selection of the best electron density map [19,29]. In a first case, assuming that we dispose of different samples of close chemical composition and different structure and that the structure of one of these samples is known, the selection is made by comparing the $\langle(\Delta\rho)^4\rangle$ obtained from the known structure with all the $\langle(\Delta\rho)^4\rangle$ values relative to any possible φ-set of the unknown structures in searching of similarity.

However, in the absence of crystallographic data relevant to other phases of similar composition, it has been well documented that the best sign combination can be selected in the φ-set list by comparing the $\langle(\Delta\rho)^4\rangle$ values with a reference $\langle(\Delta\rho)^4\rangle^*$ calculated from the chemical properties of the sample [19]. On the basis of the assumption that a complete segregation between polar (and water, if present) and hydrocarbon portions occurs, the unit cell of the lipid sample can be divided into two complementary volumes, so that the $\langle(\Delta\rho)^4\rangle^*$ can be expressed [19] in terms of the average of the powers of $\rho(r)$ over the two volumes and of the volume concentrations $c_{v,pol}$ and $c_{v,par}$:

$$c_{v,pol} = 1 - c_{v,par} \tag{4}$$

$$c_{v,pol}\langle\rho_{pol}\rangle + c_{v,par}\langle\rho_{par}\rangle = 0$$

$$c_{v,pol}\langle\rho_{pol}\rangle^2 + c_{v,par}\langle\rho_{par}\rangle^2 = 1 - (\epsilon_2)^2$$

$$c_{v,pol}\langle\rho_{pol}\rangle^4 + c_{v,par}\langle\rho_{par}\rangle^4 = \langle(\Delta\rho)^4\rangle^* - (\epsilon_4)^2.$$

$(\epsilon_2)^2$ and $(\epsilon_4)^2$ are positive numbers defined by:

$$(\epsilon_m)^2 = c_{v,pol}(\langle\rho_{pol}^m\rangle - \langle\rho_{pol}\rangle^m) + c_{v,par}(\langle\rho_{par}^m\rangle - \langle\rho_{par}\rangle^m)$$

When the electron density is constant over the two volumes, or when the fluctuations $|\rho_{par}(r) - \langle\rho_{par}\rangle|$ and $|\rho_{pol}(r) - \langle\rho_{pol}\rangle|$ are smaller if compared with $|\langle\rho_{par}\rangle - \langle\rho_{pol}\rangle|$, then $(\epsilon_2)^2$ and $(\epsilon_4)^2$ are equal to zero, and the system of Eqs. (4) can be solved:

$$\langle(\Delta\rho)^4\rangle^* = 1/[c_{v,pol}(1 - c_{v,pol})] - 3 \tag{5}$$

This relationship gives the second criterion to solve the phase problem.

It is interesting to analyse the variation of $\langle(\Delta\rho)^4\rangle^*$ with chemical composition. As reported in Fig. 5, in the intermediate region the curve goes towards the minimum, reaching the value of 1.0 for a polar volume concentration of 0.5, while for small polar (or paraffinic, as the curve is symmetrical) volume concentrations, the $\langle(\Delta\rho)^4\rangle^*$ value strongly increases. This behaviour has indeed been observed in lyotropic structures [19,29–31] (see also Ref. [32]). In particular, in the case of systems characterised by fairly smooth electron density distributions and with $c_{v,pol}$ equal to about 0.5, the best sign combination invariably takes a $\langle(\Delta\rho)^4\rangle$ value close to the minimum of all values compatible with the data. By contrast, in those cases where heavy atoms were present and in which the $c_{v,pol}$ resulted as practically negligible (for example, in some dried Sr myristate cubic lyotropic structures, in which Sr atoms occupy a very small cell volume fraction) the best φ-set was found to rank last, at the highest $\langle(\Delta\rho)^4\rangle$ value.

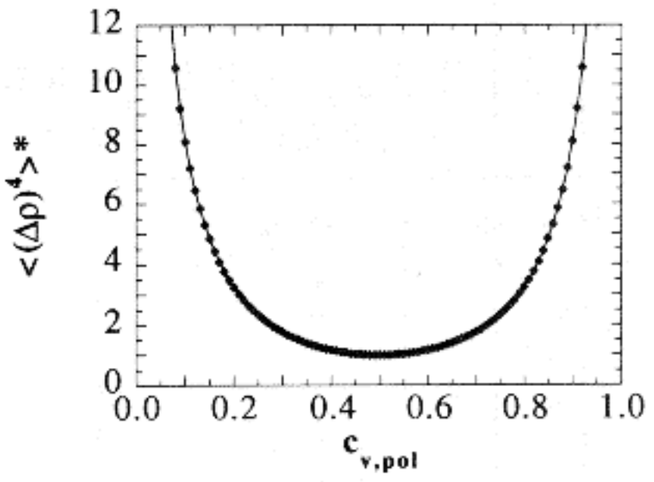

Fig. 5. Calculated dependence of the moment of order four of the normalized electron density, $\langle(\Delta\rho)^4\rangle^*$, on the polar (or paraffinic) volume concentration of the sample.

[2] In our case, the intensities are normalized such that:

$$\Sigma(I(h)) = 1$$

In this condition, the electron density profile $\Delta\rho(r)$ (the map) appears as a normalized dimensionless expression of the fluctuation of the electron density $\rho(r)$:

$$\Delta\rho(r) = [\rho(r) - \langle\rho\rangle]/[\langle\rho^2(r)\rangle - \langle\rho\rangle^2]^{1/2}$$

were $\rho(r)$ is the Fourier transform of the set of observed structure factors $F(h)$ and $\langle\rho\rangle$ is the average value of $\rho(r)$ over the unit cell volume [19]. By definition, $H(\Delta\rho)d(\Delta\rho)$ is the volume fraction of the sample over which the value of $\Delta\rho(r)$ is intermediate between $\Delta\rho$ and $(\Delta\rho + d(\Delta\rho))$. The function $H(\Delta\rho)$ is directly related to the nature of the structure elements rather than to their mutual distribution: when the structure can be decomposed into J disjointed elements $\Delta\rho_j(r)$, then $H(\Delta\rho)$ takes the form:

$$H(\Delta\rho) = \Sigma_{j=1,J} H(\Delta\rho_j)$$

and strictly fulfills the requirement of an extensive property [19]. The moment $\langle(\Delta\rho)^n\rangle$ is defined by:

$$\langle(\Delta\rho)^n\rangle = \int(\Delta\rho)^n H(\Delta\rho)d(\Delta\rho) = (1/V)\int_v(\Delta\rho(r))^n dV$$

As a consequence of the normalization procedure, the moment of the first order is equal to 0, the moment of the second order is equal to 1 and the ones of odd order are small and indiscriminating. Thus, we restrict the analysis to the moment of the fourth order.

Table 3
Lead fatty acid salts: choice of the best sign combinations

Pb stearate			Pb arachidate			Pb behenate		
Rank	φ-set	$\langle(\Delta\rho)^4\rangle$	Rank	φ-set	$\langle(\Delta\rho^4)\rangle$	Rank	φ-set	$\langle(\Delta\rho^4)\rangle$
1	+ + − − + + + − + − + − − + − + − + − + + − + −	1.359	1	+ + + − − + − + + − − + − + + + − −	1.386	1	+ + − + − − − + + − − − + −	1.374
131072	+ + − + − − − + + − − − + + − + + − + + + + − −	1.675	2048	+ + − − + − + − − − − + − + − − + −	1.736	128	+ + − + + + − − + − + − + −	1.761
262144	+ + − + − − − + + − − + − + + + + − − + + − + −	1.760	4096	+ + − + − + + + − + + + − + + + + +	1.828	256	+ + − + + − + − + − − − − +	1.865
393216	+ + + − − − + − + + − + − − − + − + − − − + + −	1.828	6144	+ + − − − + − − − + + + − − + + + −	1.896	384	+ + − − − + − + − − + + +	1.939
524288	+ + − − − + + − + − + − − − − + + + + + + + + +	1.891	8192	+ + − − + + − − + − + − − + + + + +	1.954	512	+ + − − + − − − − + + − + −	1.997
655360	+ + + − − − + − + + − + − − − + − + + + − + − +	1.943	10240	+ + + − − + − + − + − + + − − + − +	2.004	640	+ + − + + + − − − − + + − +	2.057
786432	+ + − − − + + + + − + − + − − − − + − − + + − +	1.992	12288	+ + − + − + + + − − − − − + − + − +	2.051	768	+ + − − − + + − − − + − − −	2.109
917504	+ + − + − − + + − − − − − + + − − + − − + + − +	2.033	14336	+ + − − − − + − − + − − − + − − − −	2.097	896	+ + − + + − − − − + − + + +	2.156
1048576	+ + + − − + − + + + + + − − − + − − + − + − + −	2.075	16384	+ + − − − + − − + + − + − − − − − +	2.140	1024	+ + − − + + − + − − − − − +	2.201
1179648	+ + − − − − + − − − − − − + + + − + − + − + + −	2.116	18432	+ + + − + + − − − − + − + − + + + −	2.183	1152	+ + + + − + + − − − − − + +	2.245
1310720	+ + − + − + − − + − + − + − − + + + + + − − − −	2.158	20480	+ + + − − + + + − − − + + + − − + −	2.227	1280	+ + − + + + − + − − + + +	2.285
1441792	+ + − + + − + − + + + − − − + + − + + − − + +	2.194	22528	+ + + + − + − − + + + − − + − + + −	2.271	1408	+ + + − − + − + − + − + − −	2.337
1572864	+ + + − + − − + − − + − + − + + − + + + + + +	2.242	24576	+ + + − + + − − + + − − − + + − − +	2.316	1536	+ + − + + − + + + − + − − −	2.383
1703936	+ + − − + − + + − − − − + − + − − − + − − + + −	2.284	26624	+ + + + + − − − + + − − + − − + + −	2.360	1664	+ + − + + − + + + + − − − −	2.426
1835008	+ + − − + − + + − − − − + − + − − − − + + + − −	2.326	28672	+ + − + − + − − + + + + + + − + + +	2.404	1792	+ + − − + − − − − − − − + +	2.477
1966080	+ + − + + − − − − + + + + − + − − − + − − + −	2.363	30720	+ + − + − − + + − + − + − + − − − +	2.450	1920	+ + − + + + + − − − + + + −	2.524
2097152	+ + − − + + + + − − − + + − + + − − − − − + −	2.402	32768	+ + + − + − − − − + − − − + + − − −	2.497	2048	+ + − + + − + + − − − + − +	2.573
2228224	+ + − + − − + + + − − + + − − + − − − − − − +	2.450	34816	+ + − − − + + − + − − + − + + + − +	2.545	2176	+ + − + − + − − + + − + − −	2.624
2359296	+ + + − + + − + + + + − − − + − − − − − − − +	2.500	36864	+ + + + − + + − − − − − − + + + + −	2.597	2304	+ + − + + − + − − + − + − +	2.683
2490368	+ + + − − − − + − + − + + + − − + − − − + + + +	2.553	38912	+ + − − − + + + − − − − − + − − + +	2.649	2432	+ + − − + + − − + + + − + −	2.730
2621440	+ + − + + − + + − − − + + + + − − + − + − + + +	2.610	40960	+ + + − − − − − + − + − − − + + − −	2.708	2560	+ + + + − + − + − − − − + +	2.789
2752512	+ + + + − − − + − − − + − − − + + + − − − − − −	2.674	43008	+ + − + + − + − − + + + + + + − − +	2.773	2688	+ + + + − + − − + − + + + +	2.856
2883584	+ + + − − − − + − + − + + + − − + − − − − + − −	2.741	45056	+ + + − + + + − + − − + − − + + − −	2.841	2816	+ + + − + − + − + + − − + +	2.936
3014656	+ + − + + + + + + + − − + + − + − + − − − + − − − +	2.811	47104	+ + − − − − − − − − − − + + − + − + +	2.918	2944	+ + − − − + − + + + + + − −	3.019
3145728	+ + + − + − + − + + − − + − + − + − − + − + + + +	2.913	49152	+ + + + − + − − − + − − − − − − − −	3.004	3072	+ + − − − − − − − − − + − + +	3.117
3276800	+ + + − + + − − + + − + − − − + − − − + − − − −	3.004	51200	+ + − + + + + − + + + + + − + − + −	3.106	3200	+ + − + − + − − − + − + − +	3.216
3407872	+ + + − + − + − + + − − + − + − + − − + + − + −	3.114	53248	+ + − + + − + − − + + + + + − + + +	3.225	3328	+ + + + + − + − + + − − + +	3.330
3538944	+ + + − + + + + − + + + + + − + − − + − − + −	3.321	55296	+ + + + + − + − − − − + + − − − − +	3.377	3456	+ + − − + − − + + + − + + −	3.496
3670016	+ + + + + − + − − − − + − − + + − − − + + − + −	3.551	57344	+ + + − + + + − + + − + + + + − − +	3.572	3584	+ + + − + − + − + − − − + +	3.694
3801088	+ + + + + − + − + + − − + − − + − − − + + + − −	3.811	59392	+ + + + + + − + + − − + + − + + − −	3.854	3712	+ + − − + + − + + − − + + +	3.984
3932160	+ + + + + + − + − + + + − + + + + − − − + + − −	4.268	61440	+ + + + + − + − + − + − − + + + +	4.235	3840	+ + − − − − + + + + + + − −	4.381
4063232	+ + + + − + + + + + + + − + − + + − + + + + +	5.244	63488	+ + − − − − − + + + + − − − + −	4.974	3968	+ + + + + + − + + + − + + −	5.149
4194304	+ +	13.250	**65536**	+ + + + + + + + + + + + + + + + + +	14.760	**4096**	+ + + + + + + + + + + + + +	15.840

The signs refer to the reflections reported in Table 2. The different sign combinations are ranked in order of increasing $\langle(\Delta\rho)^4\rangle$. The best φ-set is bold-faced (compare with the references $\langle(\Delta\rho)^4\rangle^*$ in Table 2). Symbols and notations as in Table 1 and in the text.

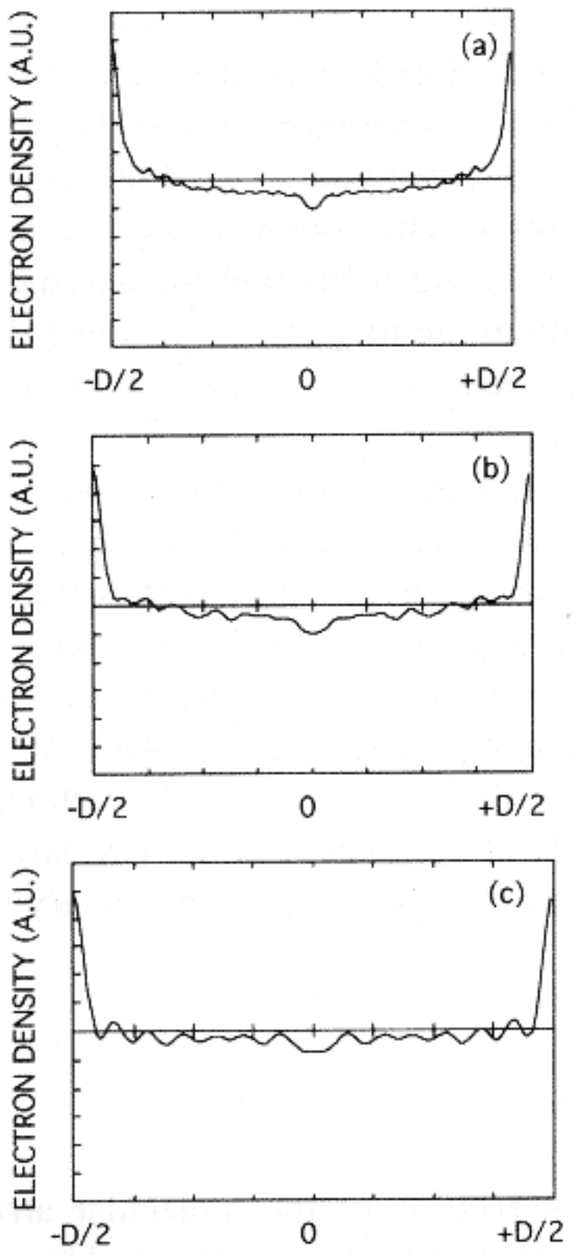

Fig. 6. Fatty acid salt LB films: electron density profiles corresponding to the sign combinations selected by using the pattern recognition approach (see text and Table 3). (a) Pb stearate; (b) Pb arachidate and (c) Pb behenate LB films. The moduli of the structure factors are reported in Table 2. The origin is at the centre of the hydrocarbon region.

3.3.1. Fatty acid salt LB films

LB films made of stearate, arachidate and behenate Pb salts have been considered in particular. The three sets of data are characterized by different experimental resolutions, equal to about 0.2 nm in the case of stearate, and better than 0.4 nm in the other two systems. As it can be seen in Table 2, in all three cases the ion, which is very electron dense with respect to the lipid molecule, occupies a very small volume fraction of the cell ($c_{v,ion}$ is of about 6%), so that sharp electron density peaks will characterize the structure. According to the results obtained in the similarly extreme situation described above, it is straightforward to predict that the parameter $\langle(\Delta\rho)^4\rangle$ corresponding to the best electron density map will take the highest value of all values compatible with the experimental data.

We also calculated the reference $\langle(\Delta\rho)^4\rangle^*$. Considering the quite similar electron densities of the CH_3, CH_2 and COO^- groups with respect to the Pb ion, we substitute in Eq. (5) the $c_{v,pol}$ value with $c_{v,ion}$. The results are reported in Table 2. Table 3 shows a partial list of sign combinations ranked according to increasing $\langle(\Delta\rho)^4\rangle$: the comparison with the reference values of Table 2 confirms that in all the three cases the best map is the one ranking last. The corresponding electron density maps are reported in Fig. 6.

The excellent agreement between the selected maps and the well known structure of fatty acid salt LB films [11] is the most convincing argument in support of the final result. From the maps it is possible to measure directly the dimensions of polar and paraffinic layers and obtain evidence of the localization of cations (there is an unsplit narrow maximum consistent with the arrangement of the metal atoms) and of the contact of chains on adjacent monolayers. It also appears that the hydrocarbon chains are rigid, stiff and tilted with respect to the layer plane.

A last point must be stressed. The theoretical $\langle(\Delta\rho)^4\rangle^*$ are higher than the maxima reported in Table 3. These differences could be ascribed to truncation effects in the Fourier analysis which affect the calculated $\langle(\Delta\rho)^4\rangle$. In particular, we observed that the difference between the reference $\langle(\Delta\rho)^4\rangle^*$ and the calculated maxima increases as far as the resolution is arbitrarily cut. In the case of Pb arachidate, for example, if only the first 12 reflections over the 18 observed are kept (i.e. if the resolution is reduced from 0.29 to 0.43 nm), the highest $\langle(\Delta\rho)^4\rangle$ was reduced from 14.76 to 11.90, at a value still lower than the theoretical $\langle(\Delta\rho)^4\rangle^*$. Moreover, the decrease of the observed intensities with increasing h is roughly comparable with that expected from an ideal step function, so that the distortion of the first kind as well as the temperature factor have been neglected in the estimation of the structure factors [20,23,24]. However, it is evident that the effect of these simplifications could also contribute to the observed differences.

3.3.2. Bipolar lipid LB films

Concerning the Phospho 2 LB film, we report in Table 2 the polar volume concentration and the $\langle(\Delta\rho)^4\rangle^*$ calculated by using Eq. (5). The screening in the φ-set list is done by searching for a similarity between the $\langle(\Delta\rho)^4\rangle$ relative to all the possible electron density maps compatible with the experimental data and the theoretical parameter. The possible sign combinations are reported in Table 4. Considering the expected value, it is evident that the solution ranking at position 5 must be considered as the best one. The corresponding electron density distribution is reported in Fig. 7.

This electron density map appears to be very reasonable. In particular, the map indicates a layered packing of the bipo-

Table 4
Bipolar Phospho 2 lipid: choice of the best sign combination

Rank	φ-set	$\langle(\Delta\rho)^4\rangle$
1	+ + − − +	1.493
2	+ + − − −	1.539
3	+ + − + −	1.719
4	+ + − + +	1.857
5	**+ + + − −**	**1.995**
6	+ + + − +	2.307
7	+ + + + −	2.484
8	+ + + + +	3.077

The signs refer to the reflections reported in Table 2. The different sign combinations are ranked in order of increasing $\langle(\Delta\rho)^4\rangle$. The best φ-set is bold-faced (compare with the reference $\langle(\Delta\rho)^4\rangle^*$, see Table 2). Other symbols and notations as in Table 1 and in the text.

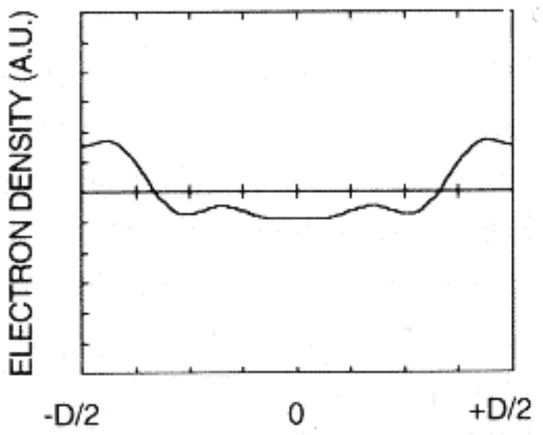

Fig. 7. Phospho 2 bipolar lipid LB film: electron density profile corresponding to the sign combination selected by using the pattern recognition approach (see text and Table 4). The moduli of the strucure factors are reported in Table 2. The origin is at the centre of the hydrocarbon region.

lar molecules and shows a quite smooth electron density in the paraffinic region, the thickness of which exactly corresponds to the thickness calculated from the paraffinic volume concentration and the unit cell parameter. Moreover, the density maxima consistent with the arrangement of the lipid polar heads are resolved; the polar group are arranged at a distance of about 0.6 nm from one another.

In order to verify this result, we calculate the electron density maps relative to the two possible structural models shown in Figs. 3(a) and 3(b). It is obvious, in fact, that the model depicted in the Fig. 3(c) can be immediately rejected, because the selected profile reported in Fig. 7 does not show the increase of electron density in the central position which could be expected considering the location of the polar groups. The two structures reported in Figs. 3(a) and 3(c) have then been represented as steep models by using electron density data and volumes reported by Gulik et al. [34] as indicated in Fig. 8. The intensities of the Bragg peaks corresponding to these two models have been then calculated at 1 nm of resolution. The obtained electron density maps are also reported in the Fig. 8. For both models, the corresponding sign combinations are identical to the one selected by using the $\langle(\Delta\rho)^4\rangle$ method: this finding strongly supports the obtained result.

One point must be stressed. As we are referring to low resolution data, the maps calculated for both models are very similar to that obtained from the experimental data (compare Figs. 7 and 8), although the particular shape of the paraffinic region in the experimental map and the very small intensity of the $h=4$ Bragg peak suggest that the U-shaped molecular conformation is the more probable. Nevertheless, we cannot unambiguously choose between the two structural models. High resolution data appear to be necessary to confirm this indication.

4. Conclusion

The characterization of the molecular arrangement and packing is an important step in the problem of producing, investigating and using LB films [24]. Considering in particular the technological and biological growing interest for LB films which exhibit new properties linked to particular

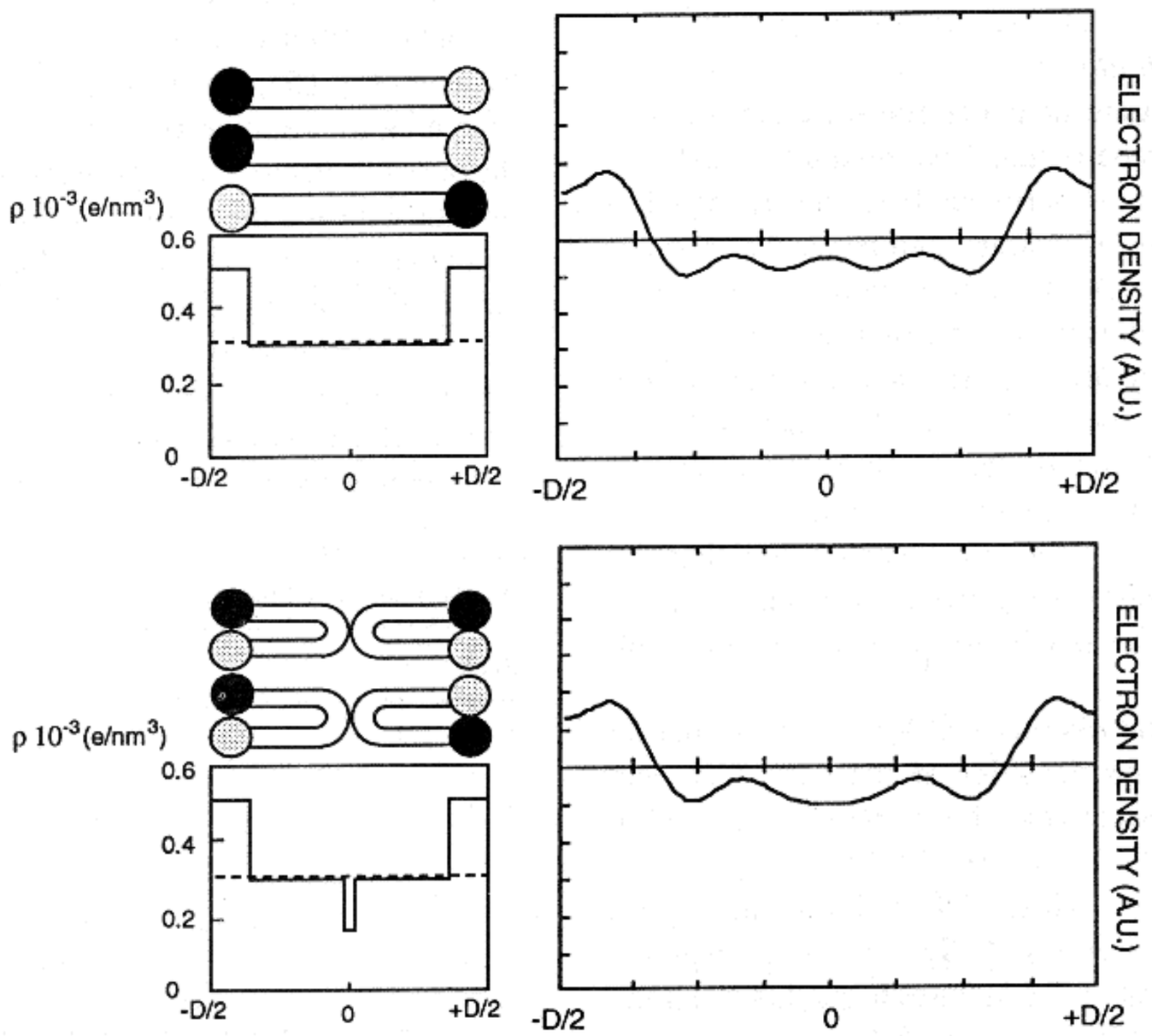

Fig. 8. Bipolar lipid LB film: step models and electron density maps relative to the two structural models reported in the Figs. 3(a) and 3(b) calculated at resolution of about 1 nm. Upper frame: fully extended centro-symmetric conformation. The corresponding structure factors are the following: $F(1)=0.580$; $F(2)=0.327$; $F(3)=0.055$; $F(4)=-0.143$; $F(5)=-0.184$. Lower frame: U-shaped conformation. The corresponding structure factors are the following: $F(1)=0.607$; $F(2)=0.267$; $F(3)=0.103$; $F(4)=-0.188$; $F(5)=-0.126$.

molecular types or to a peculiar construction accomplished at the molecular level in one dimension, it appears interesting to improve classical structural techniques and to test new approaches to solve those problems which, in correspondence with the increase on the structure complexity, become more and more complex. Within this purpose, in the present work we discuss the structural analysis of two different types of LB films made of fatty acid salts and of bipolar lipids extracted from thermoacidophilic archaeon *Sulfolobus solfataricus*. Concerning the analysis of the diffracted intensities, we apply a pattern recognition approach, which gives a direct solution to the phase problem without any subjective assumption about a presumed structure.

The results can be summarised as follows. In the case of the series of fatty acid salts, once the symmetry and the unit cell dimension have been determined, the electron density distributions across the layers can be calculated. In particular, we demonstrate that little easily accessible chemical information (namely the volume concentration in the unit cell of the heavy atoms and the electron densities of the polar and paraffinic media) give the criterion to select the best sign combination.

The same approach is then applied to study the bipolar lipid films. The limited order on the produced LB film structure results in a X-ray diffraction pattern characterized by only 4–5 Bragg peaks. As before, easily accessible chemical information (namely the volume concentration of the polar lipid headgroups) gives the criterion to chose the best electron density distribution. The selected electron density provides information about the film structure. In agreement with some recent results obtained by surface pressure isotherm measurements and X-ray reflectivity experiments [11,25], the whole of the results and the comparison with step models suggest that in the LB film the bipolar lipid molecules assume the U-shaped conformation.

As a final comment, we underline the first and very successful application of the pattern recognition approach to diffraction data at about 0.2 nm of resolution. As these results have been obtained without assumption about the structure, we are extending this approach to solve specific LB film crystallographic problems, as in particular the structure determination of superlattices or non-centro symmetric polar Z-or X-type LB films [35].

Acknowledgements

This work has been developed within the framework of National Program of Research on Bioelectronics of the Italian Ministry of University and Scientific and Technological Research. PM acknowledges the CNR (Italy) and the Russian Academy of Sciences for financial support during his stay in Moscow.

References

[1] B. Blodgett and I. Langmuir, *Phys. Rev., 51* (1937) 964.
[2] D.M. Tiede, *Biochem. Biophys. Acta, 811* (1985) 357.
[3] R. Kjaer, J. Als-Nielsen, C.A. Helm, L.A. Laxhuber and H. Mohwald, *Phys. Rev. Lett., 58* (1987) 2224.
[4] C.L. Honeybourne, *J. Phys. Chem. Solids, 48* (1987) 109.
[5] A.S. Dhindsa, G.H. Davies, M.R. Bryce, J. Yarwood, J.P. Lloyd, M.C. Petty and Yu.M. Lvov, *J. Mol. Electron., 5* (1989) 135.
[6] J.D. Earls, I.R. Peterson, G.J. Russell, I.R. Girling and N.A. Cade, *J. Mol. Electron., 2* (1986) 85.
[7] A. Ruaudel-Teixier and A. Barraud, *J. Chem. Phys., 84* (1987) 469.
[8] P.S. Vincett and G.G. Roberts, *Thin Solid Films, 68* (1980) 135.
[9] G.G. Roberts, *Adv. Phys., 34* (1985) 475.
[10] V.V. Erokhin, R.L. Kaayushina, Yu.M. Lvov and L.A. Feigin, *Studia Biophys., 132* (1989) 97.
[11] T.S. Berzina, V.I. Troitsky, A. Riccio, M. De Rosa, S. Dante, E. Maccioni, F. Rustichelli, P. Accossato and C. Nicolini, *Mater. Sci. Eng. C,* in press.
[12] C.R. Woese, O. Kandler and M.L. Wheelis, *Proc. Natl. Acad. Sci. USA, 87* (1990) 4576.
[13] O. Kandler, in M.J. Danson, D.W. Hough and G.G. Lunt (eds.), *The Archaebacteria: Biochemistry and Biotechnology*, Portland Press, London, 1992, p. 195.
[14] M. De Rosa and A. Gambacorta, *Prog. Lipid Res., 27* (1988) 153.
[15] M. Kates, in M.J. Danson, D.W. Hough and G.G. Lunt (eds.) *The Archaebacteria: Biochemistry and Biotechnology*, Portland Press, London, 1992, p. 51.
[16] G.D. Sprott, *J. Bioenerg. Biomembr., 24* (1992) 555.
[17] M. De Rosa, A. Gambacorta, B. Nicolaus and J.D. Bu'Lock, *Phytochemistry, 19* (1980) 827.
[18] S.L. Lo, C.E. Montague and E.L. Chang, *J. Lipid Res., 30* (1989) 944.
[19] V. Luzzati, P. Mariani and H. Delacroix, *Makromol. Chem. Macromol. Symp., 15* (1988) 1.
[20] M. von Frieling and H. Badaczek, *Acta Crystallogr., A46* (1990) 227.
[21] M. De Rosa, A. Gambacorta and J.D. Bu'Lock, *J. Gen. Microbiol., 86* (1975) 156.
[22] M. De Rosa, S. De Rosa, A. Gambacorta and J.D. Bu'Lock, *Phytochemistry, 19* (1980) 249.
[23] A.E. Blaurock and C.R. Worthington, *Biophys. J., 6* (1966) 305.
[24] L.A. Feigin, Yu.M. Lvov and V.I. Troitsky, in I.M. Khalatnikov (ed.), *Soviet Scientific Reviews, Section A, Physics Reviews*, USSR Academy of Sciences, Moscow, 1989, Vol. 11, p. 287.
[25] S. Dante, M. De Rosa, H. Franz, E. Maccioni, C. Nicolini, A. Riccio and F. Rustichelli, in press.
[26] *International Tables for X-ray Crystallography*, Kynoch Press, Birmingham, 1952.
[27] B. Belbeoch, M. Rouilliay and M. Tournarie, *Thin Solid Films, 134* (1990) 89.
[28] M. Mulè, E. Stussi, D. De Rossi, T.S. Berzina and V.I. Troitsky, *Thin Solid Films, 237* (1994) 225.
[29] P. Mariani, V. Luzzati and H. Delacroix, *J. Molecular Biol., 204* (1988) 165.
[30] P. Mariani, A. Colotto and G. Albertini, *Chem. Phys. Lipids, 55* (1990) 283.
[31] R. Vargas, P. Mariani, A. Gulik and V. Luzzati, *J. Molecular Biol., 225* (1992) 137.
[32] V. Luzzati, H. Delacroix, A. Gulik, P. Mariani and R. Vargas, *Structural and Biological Roles of Non-Bilayer forming Lipids*, in press.
[33] A. Tardieu, *Ph.D. Thesis*, Université Paris Sud, 1972.
[34] A. Gulik, V. Luzzati, M. De Rosa and A. Gambacorta, *J. Molecular Biol., 182* (1985) 131.
[35] P. Mariani and H. Delacroix, in press.